RESEARCH ARTICLE

WILEY

Anterior cingulate cortex differently modulates frontoparietal functional connectivity between resting-state and working memory tasks

Xin Di[1,2] 🄳 | Heming Zhang[1] | Bharat B Biswal[1,2] 🄳

[1]School of Life Sciences and Technology, University of Electronic Science and Technology of China, Chengdu, China

[2]Department of Biomedical Engineering, New Jersey Institute of Technology, Newark, New Jersey

Correspondence
Bharat B. Biswal, PhD, 607 Fenster Hall, University Height, Newark, NJ, 07102.
Email: bbiswal@yahoo.com

Abstract

The brain frontoparietal regions and the functional communications between them are critical in supporting working memory and other executive functions. The functional connectivity between frontoparietal regions are modulated by working memory loads, and are shown to be modulated by a third brain region in resting-state. However, it is largely unknown whether the third-region modulations remain the same during working memory tasks or were largely modulated by task demands. In the current study, we collected functional MRI (fMRI) data when the subjects were performing n-back tasks and in resting-state. We first used a block-designed localizer to define the frontoparietal regions that showed higher activations in the 2-back than the 1-back condition. Next, we performed physiophysiological interaction (PPI) analysis using left and right middle frontal gyrus (MFG) and superior parietal lobule (SPL) regions, respectively, in three continuous-designed runs of resting-state, 1-back, and 2-back conditions. No regions showed consistent modulatory interactions with the seed pairs in the three conditions. Instead, the anterior cingulate cortex (ACC) showed different modulatory interactions with the right MFG and SPL among the three conditions. While the increased activity of the ACC was associated with decreased functional coupling between the right MFG and SPL in resting-state, it was associated with increased functional coupling in the 2-back condition. The observed task modulations support the functional significance of the modulations of the ACC on frontoparietal connectivity.

KEYWORDS

anterior cingulate cortex, higher-order brain connectivity, modulatory interaction, physiophysiological interaction, working memory

1 | INTRODUCTION

Working memory involves distributed brain regions, most prominently the bilateral frontoparietal network (Barch et al., 2013; Mencarelli et al., 2019; Owen, McMillan, Laird, & Bullmore, 2005).

Understanding the functional integrations among the distributed regions is critical to understand the neural implementations of working memory. The bilateral frontoparietal regions show high correlations even in resting-state, thus forming lateralized frontoparietal networks when using data driven methods such as independent

component analysis (ICA; Beckmann, DeLuca, Devlin, & Smith, 2005; Biswal et al., 2010; Di & Biswal, 2013). Because of the presence of functional connectivity during resting-state, it would be more critical to investigate the relative changes of functional connectivity during working memory tasks. Electroencephalogram (EEG) studies typically show increased connectivity in the theta band and reduced connectivity in the alpha band between frontoparietal regions (Babiloni et al., 2004; Dai et al., 2017; Sauseng, Klimesch, Schabus, & Doppelmayr, 2005). As blood-oxygen-level dependent (BOLD) signals measured by functional MRI (fMRI), the signal synchronizations between some of the frontoparietal regions were found to be reduced during higher working memory load condition compared with control condition, although these regions were more activated in the same contrast (Di & Biswal, 2019).

In addition to task modulations, functional connectivity between two regions might also be modulated by a third region (Di & Biswal, 2015a; Friston et al., 1997). In the context of working memory, some executive or distractive signals from other brain region might facilitate or disrupt the functional communications between frontoparietal regions. This will result in higher-order interactions among three brain regions, which can be studied using physiophysiological interaction (PPI) model (Di & Biswal, 2013; Friston et al., 1997) or nonlinear dynamic causal modeling (Stephan et al., 2008). Several studies have been performed to characterize the modulatory interactions in resting-state (Di & Biswal, 2013, 2014, 2015a, 2015b). Particularly, we defined the frontoparietal regions of interest (ROIs) by using ICA and performed PPI analysis on the left and right frontoparietal ROIs, respectively (Di & Biswal, 2013). We identified several medial frontal and parietal regions that showed negative modulatory interaction with the frontoparietal ROIs, indicating that the increases of activity of these regions are accompanied by reduced frontoparietal functional connectivity. However, this analysis was only performed in resting-state. It remains unclear whether similar effects would be shown in task conditions, or it could alter significantly upon task demands.

The goal of the current study is to examine whether modulatory interactions of the frontoparietal regions are modulated by task demands. We adopted a n-back paradigm with varying working memory loads where the bilateral frontoparietal regions are consistently activated (Barch et al., 2013; Owen et al., 2005). We first used a block-designed localizer to identify the frontoparietal regions that showed higher activations during the 2-back than the 1-back condition. We then performed PPI analysis by using the frontal and parietal ROIs in three separate continuous task conditions, that is, resting-state, 1-back, and 2-back conditions. We examined two competing hypotheses. First, there are modulatory interactions of a third region with the two ROIs, and the effects are consistent across the conditions. In contrast, there may be modulatory interactions of a third region with the two ROIs, but the effects highly depend on the task conditions. We performed conjunction analysis to identify brain regions that may fulfill the first hypothesis, and performed repeated measure one-way ANOVA to find regions that may fulfill the second hypothesis.

2 | METHODS

2.1 | Subjects

Fifty participants (26 females) were recruited for the current study. The mean age was 22.34 years (19–24 years, *SD* = 1.303). One subject was removed because of a large head motion during MRI scan. All participants reported normal auditory and normal or corrected-to-normal visual acuity, and were free of neurological or psychiatric problems. All study procedures were carried out with written informed consent of each subject. Each subject received honorarium of 200 RMB for participation. The study was approved by the institutional review board.

2.2 | Study procedure

At the beginning of the MRI scan session, the participants underwent a resting-state fMRI scan (8 min 30 s). The participants were instructed to lay still with eyes open and staring at a white cross fixation on a dark background. Four working memory task runs were then performed with the following order: Two block-designed runs with both 1-back and 2-back condition in each run (3 min 46 s each), one continuous run of 1-back condition (5 min 10 s), and one continuous run of 2-back condition (5 min 10 s). A high-resolution anatomical T1-weighted MRI was scanned at the end of the MRI session.

2.2.1 | N-back task

The n-back task tested the participants' working memory on the spatial locations of letters presented on the screen. A white cross fixation was presented at the center of the dark screen throughout the experiment. A random letter would be presented in 1 of the 4 visual field quadrants around the fixation. In a n-back task condition (*n* = 1 or 2), participants were asked to press the left button with the left thumb when the location of the current letter matched with the one presented "*n*" item(s) back, and pressed the right button with the right thumb when it did not match with the one presented "*n*" item(s) back. The letter stimulus was presented for 500 ms, followed by an inter-stimulus interval of 2,500 ms. One-third of the total trials were "matches". Participants were instructed to focus only on the location of the letter, but not on the letter itself, and to classify the stimuli as accurately and quickly as possible. Visual stimuli were presented and responses were collected using E-Prime (Psychology Software Tools).

The n-back task procedures were designed in two ways. First, in the two localizer runs, the n-back stimuli were presented as separate blocks of 1-back or 2-back conditions. Each run started with a 10 s fixation. Then, each of the block consisted of eight trials (24 s), with a 24-s fixation period intercepted between the task blocks. The orders of task blocks of the two runs were "ABBA" and "BAAB", respectively. As a result, each run lasted for 3 min and 46 s. Second, in the two continuous runs, the n-back trials were presented continuously without a

long fixation period between them. The 1-back and 2-back conditions were allocated in two separate runs. Each run started with a 10 s fixation period, and followed by 100 trials. Each run lasted for 5 min and 10 s.

2.2.2 | MRI scanning parameters

MRI data were acquired on a 3 T GE Signa Scanner (General Electric Company, Milwaukee, WI) in functional MRI center at the University of Electronic Science and Technology of China. An eight-channel head coil was used. The scanning parameters for the fMRI were: TR (repetition time) = 2,000 ms; TE (echo time)) = 30 ms; flip angle = 90°; FOV (field of view) = 240 × 240 mm²; matrix size = 64 × 64; axial slice number = 42 with slice thickness = 3 mm and gap = 0). As a result, each resting-state run consisted of 255 images, each block-designed run consisted of 113 images, and each continuous task run consisted of 155 images. Structural T1-weighted images were acquired using the following parameters: TR = 6 ms; TE = Minimum; TI = 450 ms; flip angle = 12°; FOV = 256 × 256 mm²; matrix size = 256 × 256; sagittal slice number = 156 with slice thickness = 1 mm.

2.3 | FMRI data analysis

2.3.1 | Preprocessing

FMRI images were processed using SPM12 (SPM, RRID: SCR_007037; https://www.fil.ion.ucl.ac.uk/spm/) under MATLAB environment (R2017b). The anatomical image of each subject was segmented into gray matter (GM), white matter (WM), cerebrospinal fluid (CSF), and other brain tissue types, and normalized into standard Montreal Neurological Institute (MNI) space. The first five functional images of each run were discarded from analysis. The remaining images were realigned to the first image of each run, and coregistered to the anatomical image. The deformation field images obtained from the segmentation step were used to normalize all the functional images into MNI space, with a resampled voxel size of 3 × 3 × 3 mm³. All the images were spatially smoothed using an 8 × 8 × 8 mm³ Gaussian kernel.

We calculated frame-wise displacement for the translation and rotation directions to reflect the amount of head motions (Di & Biswal, 2015a). We adopted the threshold of maximum frame-wise displacement of 1.5 mm or 1.5° (half voxel size), or mean frame-wise displacement of 0.2 mm or 0.2°. The subjects with any of the five runs exceeding the threshold would be removed from the analysis. As a result, one subject's data were discarded.

2.3.2 | Activation analysis of the block-designed runs

We first defined a general linear model (GLM) to perform voxel-wise analysis on the block-designed runs to identify task activations between the 2-back and 1-back conditions. The two runs were modeled together with their own task regressors, covariates, and constant terms. The 2-back and 1-back conditions were defined as two box-car functions convolved with canonical hemodynamic response function (HRF). The first eigenvector of the signals in the WM and CSF, respectively, and 24 head motion regressors (Friston, Williams, Howard, Frackowiak, & Turner, 1996) were added as covariates. There was also a high-pass filter (1/128 Hz) implicitly implemented in the GLM. After model estimation, a contrast of 2-back – 1-back was defined to reflect the differences of activations between the two conditions.

Group level analysis was performed using one-sample t test GLM with the contrast images of 2-back versus 1-back as dependent variables. Activated clusters were first identified using a threshold of $p < .001$ of a two-tailed t test (Chen et al., 2019), and the cluster extent was thresholded at cluster-level false discovery rate (FDR) of $p < .05$. Because we were interested in frontoparietal regions, we searched the peak coordinates of the resulting clusters as well as local maxima within large clusters that covered these regions. As a result, we defined bilateral middle frontal gyrus regions (MNI coordinates: RMFG, 24, 11, 56; LMFG, −24, 8, 50) and superior parietal lobule (MNI coordinates: LSPL, −18, −70, 50; RSPL, 21, −67, 53) as ROIs.

2.3.3 | PPI analysis of the continuous-designed runs

We first defined GLMs for each continuous run and subject to define ROIs. The GLMs only included the WM/CSF, head motion, and constant regressors, but did not include any task regressors. A high-pass filter (1/128 Hz) was also implicitly implemented in the GLM. After model estimation, the time series of the LMFG, LSPL, RMFG, and RSPL were extracted within spherical ROIs of 6 mm radius centered at the above mentioned MNI coordinates. All the effects of no-interests, that is, WM/CSF signals, head motion, constant, and low-frequency drifts were adjusted during the time series extraction. PPI terms were calculated for LMFG and LSPL, and RMFG and RSPL, respectively. The time series of the two ROIs were deconvolved with canonical HRF, multiplied together, and convolved back with HRF to form a PPI term (Di & Biswal, 2013; Gitelman, Penny, Ashburner, & Friston, 2003). Here we only focused on within hemisphere frontoparietal connectivity, for example, LMFG and LSPL, but excluded inter-hemisphere connectivity, for example, LMFG and RSPL. This is because usually there is no known direct anatomical connection between two different regions across hemispheres. The observed functional interactions between them, for example, LMFG and RSPL, are usually mediated by one of their corresponding regions in the opposite hemisphere, for example, RMFG or LSPL.

Next, new GLMs were built with the time series of the two ROIs and the PPI term between them for each of the ROI pairs and task conditions. Other regressors of no interests as well as the implicit high-pass filter were also included in the GLMs. The beta estimates corresponding to the interaction term were the effect of interest, which were used for the group-level analysis. We note that the beta estimates are not a function of sample size (the number of time points

in this case). Therefore, the comparisons of betas between resting-state and n-back runs are not biased by the differences in time points.

The first goal of the group analysis is to identify regions that show modulatory interaction effects consistently present in the three conditions. We performed conjunction analysis of the three conditions. First, second-level GLMs were built for the LMFG-LSPL and RMFG-RSPL analyses, respectively, using a one-way analysis of variance (ANOVA) model implemented in SPM. The GLM included three columns representing the three conditions. Second, a t contrast was defined for each condition for the positive and negative directions, respectively. Finally, we examined the conjunction effects of the three conditions for the positive and negative effects, respectively, using a threshold of one-tailed $p < .0005$ (corresponding to two-tailed $p < .001$). Cluster level FDR of $p < .05$ was used for the cluster extent threshold. Because there were no clusters survived at the two-tailed $p < .001$ threshold, we also explored lower threshold of two-tailed $p < .01$ for potential effects.

The second goal is to identify regions that showed variable modulatory interactions in the three conditions. Repeated measure one-way ANOVA model was used for this purpose, with the three conditions as three levels of a factor. The significant results of the repeated measure ANOVA indicate differences in the PPI effects between any two of the three conditions. The resulting statistical maps were thresholded at $p < .001$ with cluster-level FDR at $p < .05$.

3 | RESULTS

3.1 | Task activations in the localizer runs

We observed typical bilateral frontoparietal regions that showed higher activations during the 2-back condition compared with 1-back condition (Figure 1 and Table 1). The frontal clusters mainly covered the bilateral middle frontal gyrus and precentral gyrus. The parietal cluster mainly covered the bilateral superior parietal lobule and precuneus. The right cerebellum and left basal ganglia were also activated. There were also reduced activations in the 2-back compared with 1-back condition, mainly in the default model network and bilateral temporo-opercular regions.

3.2 | Modulatory interactions during different task conditions

We first performed conjunction analysis to identify regions that showed consistent PPI effects across the three conditions. No statistically significant clusters were found of any sizes at $p < .001$ for both the LMFG-LSPL and RMFG-RSPL analyses. We further checked the threshold of $p < .01$, and still, there were no clusters of any sizes survived.

Repeated measure one-way ANOVA showed only significant effects on the modulatory interactions of RMFG and RSPL. As shown in Figure 2 and Table 2, the only cluster mainly covered the anterior cingulate cortex (ACC). The cluster-level FDR corrected p value (.005) also survived Bonferroni correction for the two analyses (RMFG/RSPL and LMFG/LSPL). Post hoc analysis showed that the PPI effect in the ACC was positive in the 2-back condition but negative during resting-state (Figure 2b). And the differences among the three conditions were mainly driven by the differences between the 2-back condition and the other two conditions. Repeated measure one-way ANOVA of the modulatory interactions of LMFG and LSPL showed a similar cluster in the ACC. However, the cluster size could not pass the cluster-level threshold.
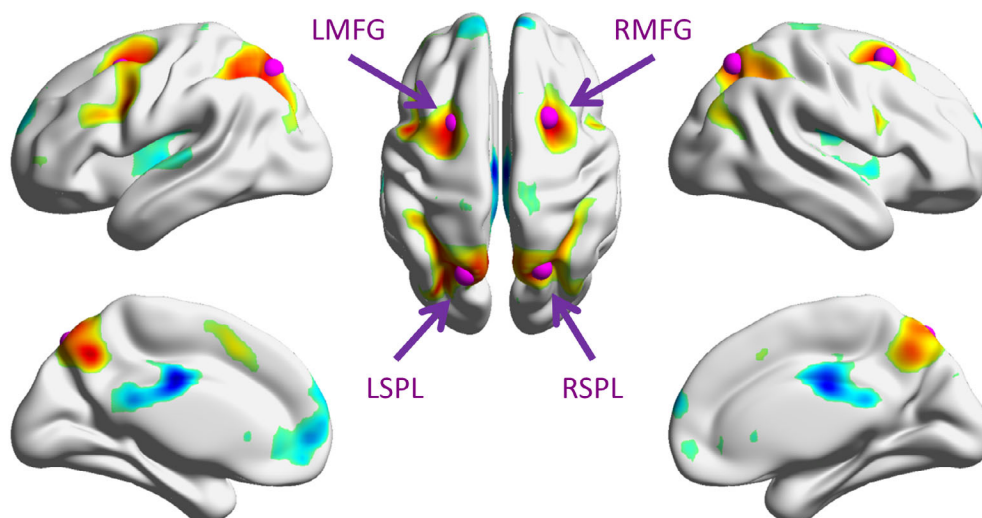

FIGURE 1 Increased (warm color) and decreased (cold color) activations in the 2-back condition compared with the 1-back condition. The map was thresholded at $p < .001$ (two-tailed) with cluster-level false discovery rate of $p < .05$. The purple spheres illustrate the four regions of interest used in the physiophysiological interaction (PPI) analysis. The surface presentation was made by using BrainNet Viewer (RRID: SCR_009446; Xia, Wang, & He, 2013). LMFG, left middle frontal gyrus; RMFG, right middle frontal gyrus; LSPL, left superior parietal lobule; and RSPL, right superior parietal lobule

TABLE 1 Clusters that showed increased or decreased activations in the 2-back condition compared with the 1-back condition in the block designed runs

		Coordinates				
p (cluster FDR)	Voxels	x	y	z	Peak T	Label
<.001	2,108	24	11	56	11.65	Right middle frontal gyrus
		−24	8	50	10.72	Left middle frontal gyrus
		−48	5	32	9.810	Left precentral gyrus
<.001	2,897	−6	−61	44	10.73	Precuneus
		−18	−70	50	10.68	Left superior parietal lobule
		21	−67	53	10.44	Right superior parietal lobule
.004	120	48	5	23	7.00	Right precentral gyrus
.003	149	27	−61	−37	6.92	Right cerebellum
		9	−73	−31	4.78	Right cerebellum
.003	136	−18	5	11	5.84	Left caudate
		−30	26	2	5.75	Left anterior insula
.038	63	−33	50	2	4.20	Left middle frontal gyrus
		−42	50	2	4.02	Left middle frontal gyrus
<.001	661	−3	−16	32	−8.73	Middle cingulate gyrus
		0	−37	20	−6.08	Posterior cingulate gyrus
		0	−28	44	−5.42	Posterior cingulate gyrus
<.001	660	39	−19	20	−6.54	Right parietal operculum
		36	−16	2	−5.56	Right posterior insula
		39	2	−1	−5.16	Right anterior insula
<.001	910	12	59	20	−6.11	Superior frontal gyrus
		−6	62	8	−5.86	Medial superior frontal gyrus
		−9	53	−1	−5.84	Medial superior frontal gyrus
<.001	498	−36	−10	−4	−5.39	Left posterior insula
		−63	−25	5	−4.73	Left superior temporal gyrus
		−39	−19	17	−4.64	Left central operculum
.037	74	21	38	−1	−5.19	Anterior cingulate gyrus

Notes. The cluster was defined as two-tailed $p < .001$, with cluster-level false discovery rate (FDR) of $p < .05$. x, y, and z coordinates are in (Montreal Neurological Institute) MNI space.

In order to better interpret the PPI effects in the ACC, we correlated the mean PPI effects in the ACC cluster with RMFC and RSPL with behavioral measures of mean reaction time and accuracy (Figure 3). The PPI effect showed a very small correlation with reaction time ($r = −.16$), and a moderate negative correlation with the accuracy ($r = −.39$). However, it can be seen in Figure 3c that there were potential outliers near the x-axis that might introduce spurious correlations. We therefore performed bootstrapping for 10,000 times to obtain a 95% confidence interval of the correlation (−0.6352, 0.0046; Figure 3d).

3.3 | Post hoc task activation analysis

Finally, we also extracted the mean task activations of the ACC in the block-designed runs (Figure 4). The ACC showed reduced activations in both the 1-back and 2-back conditions with reference to the fixation baseline. But the activations were more negative in the 2-back condition than in the 1-back condition (paired t test: $t[48] = 4.49$, $p < .001$).

4 | DISCUSSION

By comparing modulatory interactions of two key regions in working memory across three continuously designed task conditions, the current analysis identified the ACC that showed different modulatory interactions with the RMFG and RSPL in the resting-state, 1-back, and 2-back conditions. On the other hand, no regions showed consistent modulatory interactions with the frontoparietal regions across the three conditions. The activity in the ACC was positively correlated with the connectivity of RMFG and RSPL during the 2-back condition, but was negatively correlated with the connectivity of RMFG and RSPL in resting-state. Due to the nature of regression model, this is impossible to infer the directions of the modulations (Di & Biswal, 2013). However, the RMFG and RSPL were co-activated by the
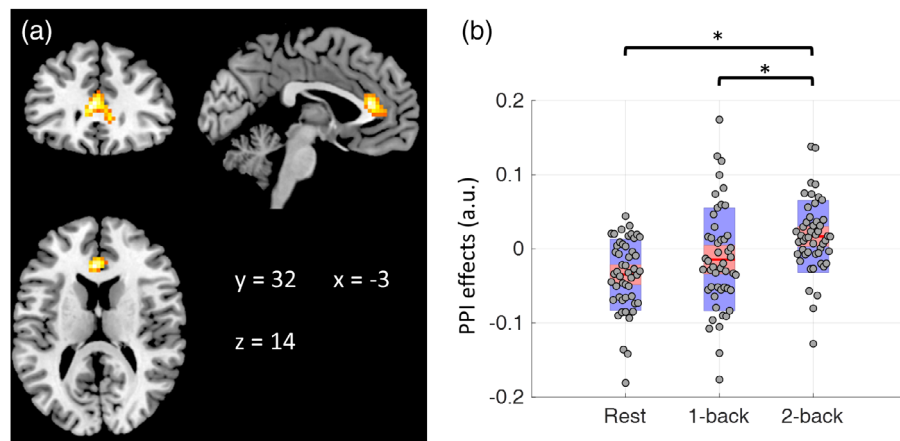
FIGURE 2 (a) Region that showed different modulatory interactions with right middle frontal gyrus (RMFG) and right superior parietal lobule (RSPL) among the three task conditions (repeated measure one-way analysis of variance, ANOVA). The map was thresholded at $p < .001$ with cluster-level false discovery rate (FDR) of $p < .05$. (b) Mean modulatory interactions of the cluster in the three conditions. The center red lines represent the mean effects, and the light red bars and light blue bars represent 95% confidence interval and standard deviation, respectively. Asterisk indicates statistical significance in post hoc pair-wise comparisons at $p < .05$. Panel b was made by using notBoxPlot (https://github.com/raacampbell/notBoxPlot). au., arbitrary unit

TABLE 2 Cluster that showed different physiophysiological interaction (PPI) effects with right middle frontal gyrus (RMFG) and right superior parietal lobule (RSPL) among the resting-state, 2-back, and 1-back conditions in the continuous runs (repeated measure one-way analysis of variance, ANOVA)

p (cluster FDR)	Voxels	Coordinates			Peak F	Label
		x	y	z		
.005	133	−3	32	14	14.94	Anterior cingulate gyrus
		9	35	5	14.82	Anterior cingulate gyrus
		3	44	−4	8.27	Anterior cingulate gyrus

Notes. The cluster was defined as $p < .001$, with cluster-level false discovery rate (FDR) of $p < .05$. x, y, and z coordinates are in (Montreal Neurological Institute) MNI space.
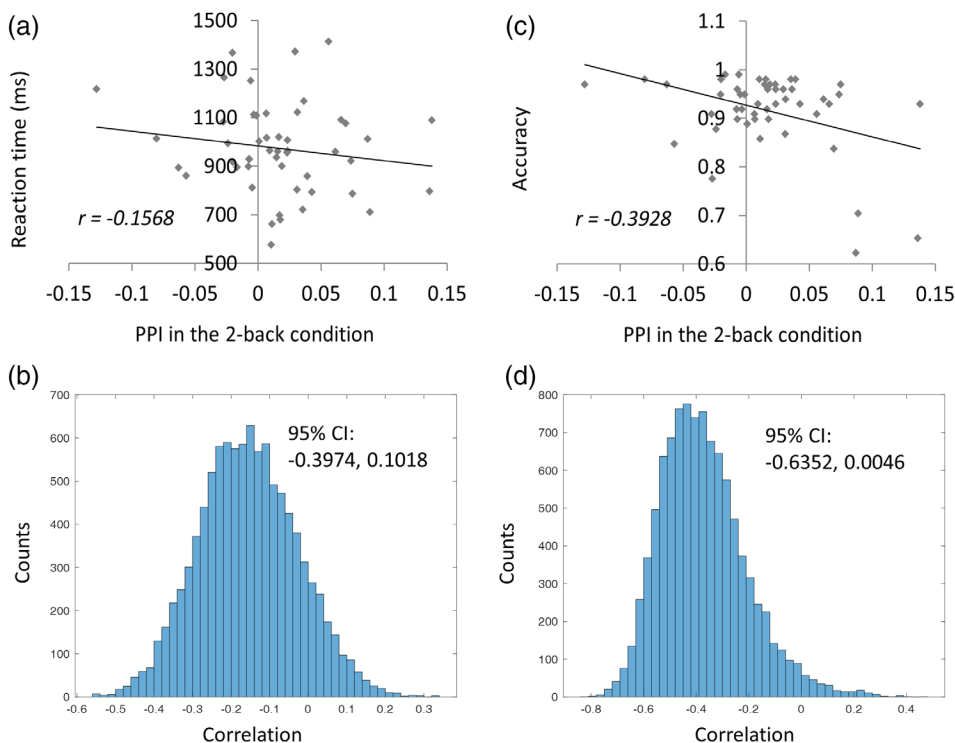

FIGURE 3 Behavioral correlates of the mean modulatory interactions in the anterior cingulate cortex (ACC) with right middle frontal gyrus (RMFG) and right superior parietal lobule (RSPL) during the 2-back continuous run. Panels a and b illustrate the relations between the modulatory interactions and reaction times and 10,000 bootstrapping distributions of the correlations. Panels c and d illustrate the relations between the modulatory interactions and accuracy and 10,000 bootstrapping distributions of the correlations
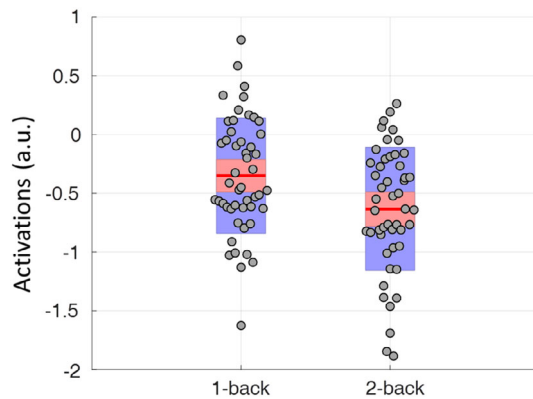
FIGURE 4 Mean task activations of the anterior cingulate cortex (ACC) cluster in the block-designed runs. The center red lines represent the mean effects, and the light red bars and light blue bars represent 95% confidence interval and standard deviation, respectively. This figure was made by using notBoxPlot (https://github.com/raacampbell/notBoxPlot). a.u., arbitrary unit

working memory task and are also considered part of the same functional network (Biswal et al., 2010; Yeo et al., 2011), while the ACC was more deactivated in the 2-back condition. We therefore incline toward interpret the results as that the ACC increase the functional connectivity between RMFG and RSPL during the 2-back condition, and reduce the functional connectivity between the RMFG and RSPL.

Due to the fact that the ACC was negatively activated in the task conditions compared with the fixation condition (Figure 4), it is likely that the ACC is part of the default mode network (Raichle et al., 2001). The current PPI results are consistent with our previous study in resting-state, which also showed some midline regions from the default mode network having negative modulatory interactions with RMFG and RSPL (Di & Biswal, 2013). The task-positive network including the frontoparietal regions and the default mode network are anti-correlated both in resting-state (Fox et al., 2005) and during task executions (Shulman et al., 1997). The current results together with our previous work (Di & Biswal, 2013) further confirm that the competing nature of the task-positive and default mode networks not only exist in first-order relationships but also in higher-order interactions.

More interestingly, current analysis found that the modulatory interactions among ACC, RMFG, and RSPL were largely modulated by task conditions. In contrast to the resting-state, the ACC showed no significant modulatory interactions in the 1-back condition, and positive modulatory interactions in the 2-back condition. The task-dependent effect is in line with some studies that have demonstrated task modulated modulatory interactions in other brain systems by using higher-order psycho-physio-physiological interaction models (Gorka, Knodt, & Hariri, 2015; Stamatakis, Marslen-Wilson, Tyler, & Fletcher, 2005). In neuronal level models, it has also been shown that higher-order interactions present only in certain task conditions (Ganmor, Segev, & Schneidman, 2011; Macke, Opper, & Bethge, 2011). Taken together, all the evidence conversely suggests that high order interactions may be sensitive to task demands.

During the 2-back condition with higher working memory loads, the signals from the ACC were associated with increased functional communications between the frontoparietal regions. One of the functions of the ACC is error detection and conflict monitoring (Bush, Luu, & Posner, 2000). Then, the ACC activity may represent error-related signals that would enhance the communications between the frontoparietal regions to maintain task performances. The brain-behavioral correlation analysis supported this interpretation. The modulatory interactions in the 2-back condition were not correlated with reaction time, but were negatively correlated with accuracy. In other words, the more errors one made, the larger the modulatory interactions were present among ACC, RMFG, and RSPL.

The current study adopted functionally defined ROIs of the MFG and SPL from a localizer for the PPI analysis. The bilateral MFGs are a little anterior to the premotor regions and posterior to the dorsolateral prefrontal cortex reported in a meta-analysis of n-back tasks (Owen et al., 2005). And the bilateral SPLs are superior and posterior to the inferior parietal lobule region reported in Owen et al. (2005). The differences may represent the discrepancies in task designs and control conditions. However, the fact that these regions showed the highest contrast between the 2-back and 1-back condition in the current localizer task support the usage of these regions to represent regions that are involved in working memory process. The frontoparietal ROIs also do not exactly match with those used in the resting-state study (Di & Biswal, 2013). However, similar to this article, the current analysis showed negative modulatory interactions in the middle line region of ACC with RMFG and RSPL in resting-state (Di & Biswal, 2013).

The current analysis adopted a ROI-based approach, with ROIs identified directly from the working memory task studied. This helped us to focus on specific brain regions that are related to the task. The whole-brain voxel-wise PPI analysis identified a region that are not a part of the frontoparietal network nor activated during the working memory tasks. It is reasonable because our previous study has shown that modulatory interactions are more likely to take place among regions from different functional networks (Di & Biswal, 2015a). There may be other brain regions that involve higher-order interactions with one of the frontoparietal regions. However, the potential interactions will increase exponentially when considering the combinations of two brain regions outside the frontoparietal network, making it difficult to do an exhaustive search based on the current sample size. Further studies may adopt the whole brain approach (Di & Biswal, 2015a) to examine the whole brain characterizations of modulatory interactions. Another limitation of the current study is that the resting-state run was always acquired at the beginning of the scan session. We designed the tasks in this way to prevent contaminations of other tasks on the resting-state, given ample evidences that task executions can alter brain signals in resting-state (Sarabi et al., 2018; Tung et al., 2013). The order effect may contribute to the observed differences in the three conditions. Further studies may add a posttask resting-state run to rule out the order effects.

In conclusion, the current analysis extended our previous analysis in resting-state and showed that the modulatory interaction among ACC and right frontoparietal regions were highly modulated by task

demands. The results may provide a new model on how error-related signals affecting the working memory process through higher-order interactions among brain regions.

CONFLICT OF INTEREST

The authors declare that there is no conflict of interest regarding the publication of this article.

AUTHOR CONTRIBUTIONS

X.D. conceived the idea. H.Z. designed the experiment and collected the fMRI data. X.D. performed the data analysis and wrote the draft. All authors discussed the results and contributed to the final manuscript.

DATA AVAILABILITY STATEMENT

The data that support the findings of this study are available on request from the corresponding author. The data are not publicly available due to privacy or ethical restrictions.

ORCID

Xin Di https://orcid.org/0000-0002-2422-9016
Bharat B Biswal https://orcid.org/0000-0002-3710-3500

REFERENCES

Babiloni, C., Babiloni, F., Carducci, F., Cincotti, F., Vecchio, F., Cola, B., … Rossini, P. M. (2004). Functional Frontoparietal connectivity during short-term memory as revealed by high-resolution EEG coherence analysis. *Behavioral Neuroscience*, 118(4), 687–697. https://doi.org/10.1037/0735-7044.118.4.687

Barch, D. M., Burgess, G. C., Harms, M. P., Petersen, S. E., Schlaggar, B. L., Corbetta, M., … Van Essen, D. C. (2013). Function in the human connectome: Task-fMRI and individual differences in behavior. *NeuroImage*, 80, 169–189. https://doi.org/10.1016/j.neuroimage.2013.05.033

Beckmann, C. F., DeLuca, M., Devlin, J. T., & Smith, S. M. (2005). Investigations into resting-state connectivity using independent component analysis. *Philosophical Transactions of the Royal Society of London. Series B, Biological Sciences*, 360(1457), 1001–1013. https://doi.org/10.1098/rstb.2005.1634

Biswal, B. B., Mennes, M., Zuo, X.-N., Gohel, S., Kelly, C., Smith, S. M., … Milham, M. P. (2010). Toward discovery science of human brain function. *Proceedings of the National Academy of Sciences of the United States of America*, 107(10), 4734–4739. https://doi.org/10.1073/pnas.0911855107

Bush, G., Luu, P., & Posner, M. I. (2000). Cognitive and emotional influences in anterior cingulate cortex. *Trends in Cognitive Sciences*, 4(6), 215–222. https://doi.org/10.1016/S1364-6613(00)01483-2

Chen, G., Cox, R. W., Glen, D. R., Rajendra, J. K., Reynolds, R. C., & Taylor, P. A. (2019). A tail of two sides: Artificially doubled false positive rates in neuroimaging due to the sidedness choice with t-tests. *Human Brain Mapping*, 40(3), 1037–1043. https://doi.org/10.1002/hbm.24399

Dai, Z., de Souza, J., Lim, J., Ho, P. M., Chen, Y., Li, J., … Sun, Y. (2017). EEG cortical connectivity analysis of working memory reveals topological reorganization in theta and alpha bands. *Frontiers in Human Neuroscience*, 11, 237. https://doi.org/10.3389/fnhum.2017.00237

Di, X., & Biswal, B. B. (2013). Modulatory interactions of resting-state brain functional connectivity. *PLoS One*, 8(8), e71163. https://doi.org/10.1371/journal.pone.0071163

Di, X., & Biswal, B. B. (2014). Modulatory interactions between the default mode network and task positive networks in resting-state. *PeerJ*, 2, e367. https://doi.org/10.7717/peerj.367

Di, X., & Biswal, B. B. (2015a). Characterizations of resting-state modulatory interactions in the human brain. *Journal of Neurophysiology*, 114(5), 2785–2796. https://doi.org/10.1152/jn.00893.2014

Di, X., & Biswal, B. B. (2015b). Dynamic brain functional connectivity modulated by resting-state networks. *Brain Structure and Function*, 220(1), 37–46. https://doi.org/10.1007/s00429-013-0634-3

Di, X., & Biswal, B. B. (2019). Toward task Connectomics: Examining whole-brain task modulated connectivity in different task domains. *Cerebral Cortex*, 29(4), 1572–1583. https://doi.org/10.1093/cercor/bhy055

Fox, M. D., Snyder, A. Z., Vincent, J. L., Corbetta, M., Van Essen, D. C., & Raichle, M. E. (2005). The human brain is intrinsically organized into dynamic, anticorrelated functional networks. *Proceedings of the National Academy of Sciences of the United States of America*, 102(27), 9673–8.

Friston, K. J., Buechel, C., Fink, G. R., Morris, J., Rolls, E., & Dolan, R. J. (1997). Psychophysiological and modulatory interactions in neuroimaging. *NeuroImage*, 6(3), 218–229.

Friston, K. J., Williams, S., Howard, R., Frackowiak, R. S., & Turner, R. (1996). Movement-related effects in fMRI time-series. *Magnetic Resonance in Medicine*, 35(3), 346–355. https://doi.org/DOI, https://doi.org/10.1002/mrm.1910350312

Ganmor, E., Segev, R., & Schneidman, E. (2011). Sparse low-order interaction network underlies a highly correlated and learnable neural population code. *Proceedings of the National Academy of Sciences of the United States of America*, 108(23), 9679–9684. https://doi.org/10.1073/pnas.1019641108

Gitelman, D. R., Penny, W. D., Ashburner, J., & Friston, K. J. (2003). Modeling regional and psychophysiologic interactions in fMRI: The importance of hemodynamic deconvolution. *NeuroImage*, 19(1), 200–207.

Gorka, A. X., Knodt, A. R., & Hariri, A. R. (2015). Basal forebrain moderates the magnitude of task-dependent amygdala functional connectivity. *Social Cognitive and Affective Neuroscience*, 10(4), 501–507. https://doi.org/10.1093/scan/nsu080

Macke, J. H., Opper, M., & Bethge, M. (2011). Common input explains higher-order correlations and entropy in a simple model of neural population activity. *Physical Review Letters*, 106(20), 208102. https://doi.org/10.1103/PhysRevLett.106.208102

Mencarelli, L., Neri, F., Momi, D., Menardi, A., Rossi, S., Rossi, A., & Santarnecchi, E. (2019). Stimuli, presentation modality, and load-specific brain activity patterns during n-back task. *Human Brain Mapping*, 40(13), 3810–3831. https://doi.org/10.1002/hbm.24633

Owen, A. M., McMillan, K. M., Laird, A. R., & Bullmore, E. (2005). N-back working memory paradigm: A meta-analysis of normative functional neuroimaging studies. *Human Brain Mapping*, 25(1), 46–59. https://doi.org/10.1002/hbm.20131

Raichle, M. E., MacLeod, A. M., Snyder, A. Z., Powers, W. J., Gusnard, D. A., & Shulman, G. L. (2001). A default mode of brain function. *Proceedings of the National Academy of Sciences of the United States of America*, 98(2), 676–682. https://doi.org/10.1073/pnas.98.2.676

Sarabi, M. T., Aoki, R., Tsumura, K., Keerativittayayut, R., Jimura, K., & Nakahara, K. (2018). Visual perceptual training reconfigures post-task resting-state functional connectivity with a feature-representation region. *PLoS One*, 13(5), e0196866. https://doi.org/10.1371/journal.pone.0196866

Sauseng, P., Klimesch, W., Schabus, M., & Doppelmayr, M. (2005). Fronto-parietal EEG coherence in theta and upper alpha reflect central

executive functions of working memory. *International Journal of Psychophysiology*, *57*(2), 97–103. https://doi.org/10.1016/j.ijpsycho.2005.03.018

Shulman, G. L., Fiez, J. A., Corbetta, M., Buckner, R. L., Miezin, F. M., Raichle, M. E., & Petersen, S. E. (1997). Common blood flow changes across visual tasks: II. Decreases in cerebral cortex. *Journal of Cognitive Neuroscience*, *9*(5), 648–663. https://doi.org/10.1162/jocn.1997.9.5.648

Stamatakis, E. A., Marslen-Wilson, W. D., Tyler, L. K., & Fletcher, P. C. (2005). Cingulate control of fronto-temporal integration reflects linguistic demands: A three-way interaction in functional connectivity. *NeuroImage*, *28*(1), 115–121. https://doi.org/10.1016/j.neuroimage.2005.06.012

Stephan, K. E., Kasper, L., Harrison, L. M., Daunizeau, J., den Ouden, H. E. M., Breakspear, M., & Friston, K. J. (2008). Nonlinear dynamic causal models for fMRI. *NeuroImage*, *42*(2), 649–662. https://doi.org/10.1016/j.neuroimage.2008.04.262

Tung, K.-C., Uh, J., Mao, D., Xu, F., Xiao, G., & Lu, H. (2013). Alterations in resting functional connectivity due to recent motor task. *NeuroImage*, *78*, 316–324. https://doi.org/10.1016/j.neuroimage.2013.04.006

Xia, M., Wang, J., & He, Y. (2013). BrainNet viewer: A network visualization tool for human brain connectomics. *PLoS One*, *8*(7), e68910. https://doi.org/10.1371/journal.pone.0068910

Yeo, B. T. T., Krienen, F. M., Sepulcre, J., Sabuncu, M. R., Lashkari, D., Hollinshead, M., ... Buckner, R. L. (2011). The organization of the human cerebral cortex estimated by intrinsic functional connectivity. *Journal of Neurophysiology*, *106*(3), 1125–1165. https://doi.org/10.1152/jn.00338.2011